Electro-Thermo-Mechanical Reliability of Recessed Barrier AlGaN/GaN Schottky Diodes Under Pulse Switching Conditions

Bhawani Shankar, Ankit Soni, and Mayank Shrivastava, *Senior Member, IEEE*

***Abstract*— Pulse reliability of AlGaN/GaN recessed Schottky diode is studied under transient overstress conditions, typically encountered in power converters. Degradation of the Schottky diode during both free-wheeling operation (high forward current injection) and reverse blocking state (high-voltage stress) is studied. Defect generation and the associated degradation were found to be uncorrelated with the nature of interface formed due to various surface treatments (at metal/GaN Schottky interface). During forward conduction, trap-assisted Schottky interface degradation is studied using on-the-fly *I–V* and *C–V* characterization under high-current stress. Under high-voltage stress, in the reverse blocking mode, mechanical strain evolution and defects generation were found to be dominant degradation modes, which are studied in detail using on-the-fly micro-Raman spectroscopy. Post-failure analysis was performed using SEM, TEM, and EDX, which reveals distinct failure signatures at the safe operating area (SOA) boundary. TCAD simulations are used to gain deeper physical insights into the observed degradation mechanism. Finally, a qualitative failure model, explaining the distinct failure physics, is presented based on observations and findings, from various electrical, optical, Raman spectroscopy, and electron microscopy investigations.**

***Index Terms*— AlGaN/GaN reliability, GaN diode, pulse switching reliability, safe operating area (SOA) reliability.**

I. Introduction

GALLIUM nitride-based power devices have shown outstanding switching performance in power electronics applications. This is inherited to the high density of 2-D electron gas (2DEG) with electron mobility and peak electron velocity better than Si and SiC. In addition to its wider bandgap and higher critical breakdown field, its lower dielectric constant makes it a promising material for high-power switching applications. Like a high-electron-mobility transistor (HEMT) for power switching, diode is an indispensable part of a typical power electronic converter, as shown in Fig. 1(a). It is used to protect power switch from reverse conduction and also used as a free-wheeling path to inductor current during the OFF-state of the switching cycle. This protection is inherently present in Si power MOSFETs in the form of a body diode; however, the same is missing in GaN HEMTs. GaN Schottky diode is an attractive option to address this. Besides, GaN Schottky diodes can also be used as an alternative to SiC- or Si-based free-wheeling diodes, attributed to its higher current conduction capability [1]. Therefore, research activities related to the GaN Schottky diode and its robustness have recently gained immense attention. Reliability of GaN Schottky diodes under steady-state stress under both ON- and OFF-states is studied in detail in the literature [2]–[6]. Under forward conduction, the diode cut-in voltage ($V_{CUT\text{-}IN}$) was degraded by the electric-field component normal to the metal/AlGaN Schottky interface while horizontal field component in channel degraded diode's ON-resistance R_{ON} [2]. Under stress in the reverse blocking mode, time-dependent failure of SiN passivation at Schottky corner limited device lifetime [3]. Trapping at AlGaN/SiN interface increased reverse leakage and R_{ON} [4]. Use of precleaned thicker passivation [5] and GaN cap [6] was suggested to improve the reliability of GaN Schottky diode in a reverse blocking regime. These works studied diode reliability in depth; however, they were restricted to steady-state current/voltage stress and do not cover the pulse switching and overstress scenarios that are typically

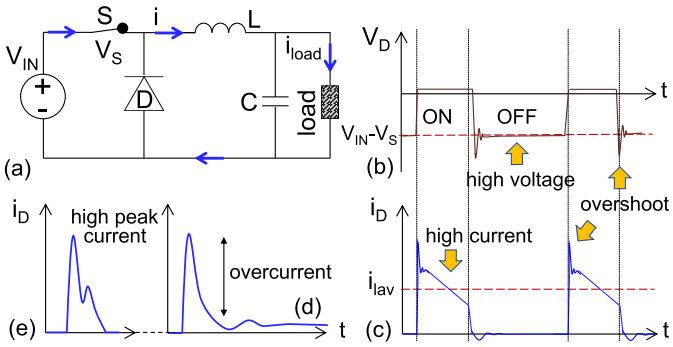

Fig. 1. (a) Schematic of DC–DC buck converter with free-wheeling diode. Diode (b) voltage and (c) current switching waveforms depicting potential overstress conditions during switching operation [10]. Waveform depicting (d) overcurrent during short-circuit event in a rectifier circuit [7] and (e) in-rush current during supply voltage interruption in an SMPS [8].

Manuscript received December 23, 2019; revised February 10, 2020; accepted March 12, 2020. Date of publication April 14, 2020; date of current version April 22, 2020. This work was supported by the Department of Science and Technology (DST), Government of India, under Project DST/TSG/AMT/2015/294. The review of this article was arranged by Editor G. Meneghesso. *(Corresponding author: Mayank Shrivastava.)*

The authors are with the Department of Electronic Systems Engineering, Indian Institute of Science, Bangalore 560012, India (e-mail: mayank@iisc.ac.in).

Color versions of one or more of the figures in this article are available online at http://ieeexplore.ieee.org.

Digital Object Identifier 10.1109/TED.2020.2981568

0018-9383 © 2020 IEEE. Personal use is permitted, but republication/redistribution requires IEEE permission.
See https://www.ieee.org/publications/rights/index.html for more information.

Authorized licensed use limited to: J.R.D. Tata Memorial Library Indian Institute of Science Bengaluru. Downloaded on October 04,2022 at 05:20:06 UTC from IEEE Xplore. Restrictions apply.

encountered in power electronic converters. For example, the following holds.

1) In a DC–DC buck converter as shown in Fig. 1(a) the free-wheeling diode-D experiences immense voltage stress (V_{IN}–V_S) [Fig. 1(b)] during the interval when transistor switch-S is ON. When the switch is OFF, the diode suffers high-current injection from the inductor [Fig. 1(c)].
2) In a diode rectifier, there can be an abrupt current overshoot during a short-circuit event, as shown in Fig. 1(d) [7].
3) A disturbance in input supply voltage in switched-mode power supply (SMPS) can lead to a high in-rush current due to the charging of capacitive filters, as shown in Fig. 1(e) [8].

Peak currents from such events can be much higher than the rated steady-state value and can overstress the device for typically ∼10 ms [7], [8]. Therefore, all these current/voltage overstress scenarios in power converters can pose serious reliability challenges to GaN Schottky diode, which has been addressed in this article. To realize a robust GaN-based Schottky diode, it is imperative to understand the diode physics and failure mechanism under pulse switching and transient stress and then tune the diode design while studying the impact of various design attributes on its robustness.

Keeping these points in mind, this article, while advancing the prior art [9], studies the reliability of recessed barrier AlGaN/GaN Schottky diode under high current and overvoltage in the pulse transient condition. Evolution of device degradation is studied using on-the-fly electrical and mechanical measurements. A failure analysis along with TCAD simulations is used to understand the degradation physics, and pulse models are proposed. This article is structured as follows. Details of device fabrication and process parameters, which are varied to engineer the quality of Schottky interface, are presented in Section II. Experimental setup that mimics the transient overstress is described in Section III. Results and observations are summarized in Section IV, while the analysis and discussions are covered in Section V. Section VI presents the distinct failure modes and associated physics. Finally, the key findings are concluded in Section VII.

II. Device Fabrication

Recessed Schottky diodes were fabricated on the AlGaN/GaN layer stack realized on Si (111), as shown in Fig. 2(a). The epi-stack was composed of AlGaN transition region, 3-μm-thick C-doped GaN buffer, 20-nm-thin AlGaN barrier layer with 20 nm of *in situ*-grown SiN passivation. Diodes 100 μm wide were processed with 5-μm anode-to-cathode spacing using UV lithography. Devices were MESA isolated on-wafer, by etching up to 180-nm GaN using Cl_2/BCl_3 chemistry in the inductively coupled plasma reactive ion etching system. AlGaN barrier was completely etched in the anode region to form direct contact with 2DEG via anode sidewalls, whereas recess depth in cathode was optimized to achieve the least contact resistance. These recesses were achieved by using the O_2/BCl_3-based digital etch technique.

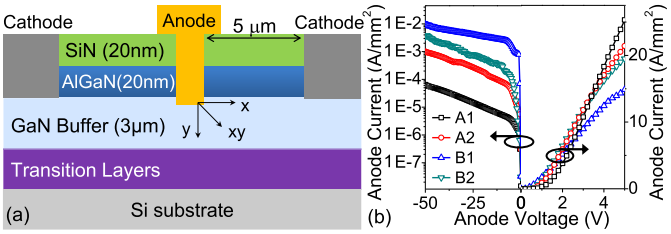

Fig. 2. (a) Schematic of AlGaN/GaN Schottky diode with recessed anode. To study the role of nature of Schottky interface on failure mechanism, the Schottky interface is processed with different types of surface treatments. (b) DC *I*–*V* characteristic of the four types of AlGaN/GaN Schottky diode under study.

TABLE I
TYPES OF SURFACE TREATMENT DONE AT SCHOTTKY INTERFACE FOR DIODES UNDER STUDY

Sample	Surface Treatment Done	Purpose	D_{it} (eV^{-1} mm^{-2})	SBH (eV)
A1	700 °C RTA (60 s) + HCl & HF dip	To reduce inhomogeneity at interface	1E8	0.59
A2	500 °C RTA (5 s) + HCl & HF dip	To reduce inhomogeneity at interface	5E8	0.57
B1	Buffer Oxide Etching (BOE)	To remove interfacial oxide	1E10	0.56
B2	No treatment		2E9	0.55

For cathode, Ti/Al/Ni/Au metal stack was deposited using *E*-beam evaporation and later annealed in N_2 ambient to form Ohmic contact with 2DEG. In our initial study, we discovered a strong correlation between the diode degradation and the trap density at the Schottky interface. Although the preliminary observations showed an increase in interface trap density (D_{it}) with stress, we wanted to further investigate whether there is any correlation between the intrinsic D_{it} and the diode failure mechanism. Keeping this in mind, in this article, diodes were processed with four types of surface treatment recipes that directly affect D_{it} at the metal/GaN Schottky interface in the anode region, as summarized in Table I. Etching of interfacial oxide increased D_{it} by one order, whereas a high-temperature anneal step reduced D_{it} by an order. In each case, surface treatment was done after etching the AlGaN barrier and before anode metal deposition. At last, anode, Ni/Au metal stack was deposited followed by annealing at 300 °C for 30 s in forming gas to form a Schottky contact with the 2DEG. Fig. 2(b) shows the DC *I*–*V* characteristic of four types of diode under study. A forward DC current up to ∼25 A/mm^2 and a reverse breakdown voltage of ∼450 V were achieved.

III. Device Characterization

A schematic of the experimental setup used in this article is shown in Fig. 3. It was developed by integrating the electrical and mechanical characterization techniques. The pulse generator applies a voltage discharge on device through a charged transmission line. The advantage of this setup is that it behaves as a voltage source in the open-load condition or high-impedance state, which is the typical scenario in the

Authorized licensed use limited to: J.R.D. Tata Memorial Library Indian Institute of Science Bengaluru. Downloaded on October 04,2022 at 05:20:06 UTC from IEEE Xplore. Restrictions apply.

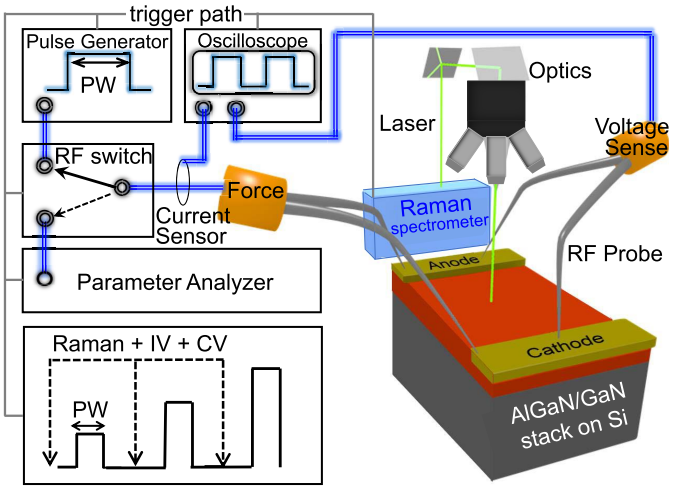

Fig. 3. Schematic of the experimental setup with integrated Raman spectrometer and sub-μs pulse generator used for on-the-fly electrical and mechanical reliability characterization of GaN Schottky diode under pulse switching stress.

diode reverse bias condition where the diode sees a high voltage from supply [Fig. 1(b)]. On the other hand, it behaves as a current source in a short-circuit or low-impedance condition, which is a typical scenario during the free-wheeling phase in power converter where the inductor injects high current into the diode in the forward mode [Fig. 1(c)]. The pulse generator was connected to the device via a high-speed RF switch. Diodes were stressed at the anode with respect to cathode using pulses of 10-ns pulsewidth (PW) with 1-ns rise time, in the forward conduction and reverse blocking mode. A delay of 1 s is introduced between two consecutive pulses to allow a reasonable time for device relaxation. The pulse current was measured using a current sensor and pulse voltage across diode was sensed using a high-impedance RF probe. Diode voltage and current waveforms were captured using a high-speed digital storage oscilloscope at 25-Gps sampling rate. Diode I–V characteristic under pulse transient stress was obtained by averaging diode voltage and current waveforms over 70%–90% time window of the captured voltage and current pulses. After each pulse, the RF switch connected DC parameter analyzer to the diode and the following were spot measured on-the-fly: 1) forward DC current (I_F) at 1 V and 2) reverse leakage current (I_R) at −10-V DC to monitor device degradation. The DC I–V and C–V characterization of diode was done at regular intervals during the stress routine to record the change, if any, in diode DC parameters. Any alteration in the Schottky interface quality due to stress was determined by recording the change in interface defect density (D_{it}). For this, the depletion capacitance was measured under reverse bias (at −2 V) with 20-kHz signal in each case. D_{it} was measured at the Schottky/GaN interface using the capacitance–conductance method [11] as $D_{\text{it}} \approx \frac{2.5}{q}\left(\frac{G_p}{\omega}\right)_{\max}$, where G_p is the conductance and ω is the frequency of applied ac signal. Schottky barrier height (SBH) was determined using the current–voltage method [11]. Any change in DC parameters of device under stress is considered as degradation. At high reverse bias voltage, mechanical strain develops across GaN due to its piezoelectric nature and

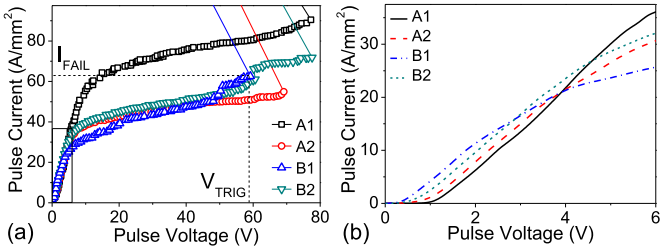

Fig. 4. (a) Pulse I–V characteristics of Schottky diode with different anode surface treatments, under current stress in the forward conduction mode. (b) Rectangle on the plot highlights the low-voltage region of characteristics.

deteriorates the device performance. Therefore, piezoelectric strain distribution in diode and its evolution under voltage stress in the reverse blocking mode was recorded across the anode–cathode region, using on-the-fly 2-D Raman mapping at 532-nm wavelength. A right shift in E_{2-H} (567.5 cm^{-1}) GaN Raman peak indicates the presence of compressive strain and vice versa [12]. All measurements were done at room temperature. Post stress, failure analysis using TEM and SEM along with EDX was performed to gain physical and chemical insight into the failure mechanism(s) involved.

IV. Experiments and Observations

A. High-Current Stress During Forward Conduction

Pulse stress was applied at anode and increased until the diode faced catastrophic failure. Fig. 4(a) shows the I–V characteristics of diodes with different surface treatments performed at the Schottky interface under forward conduction stress. All diodes under stress showed linear characteristics from cut-in voltage ($V_{\text{CUT-IN}}$) till 7 V. However, the characteristics partially saturated beyond 10 V. Subsequently, a snapback was triggered (at V_{TRIG}), which resulted in catastrophic failure. The onset of snapback is used as the failure threshold (I_{Fail}). It should be noted that during the normal operation, the diode stays in a linear region when the injected current is of the order of diode current rating (∼30 A/mm^2 under pulse) or lower, exhibiting low voltage drop (<7 V), as shown in Fig. 4(a). However, in certain load mismatch conditions, there can be overcurrent injection, as highlighted in Section I. The moment that the diode encounters current stress greater than its rated current, the diode current saturates very quickly as shown in Fig. 4(a), and the voltage drop across diode increases to a high value (up to 80 V) with an incremental change in current.

Fig. 4(a) also shows that the pulse I–V behavior of GaN diodes remains unchanged with Schottky interface treatment. Diode-A1, which was annealed to high temperature for a longer time, had shown a higher failure threshold (∼1.6×) when compared to the untreated diode-B2 with no change in V_{TRIG}. On the other hand, diode-B1, which was treated to remove interfacial oxide, showed the lowest V_{TRIG} compared with untreated diode-B2. A closer look at the linear region of pulse I–V characteristics in Fig. 4(b) reveals that $V_{\text{CUT-IN}}$ increases in the following order; diode-B1 < B2 < A2 < A1. On one hand, oxide etching in diode-B1 removed interfacial oxide and eliminated unwanted drop across it which reduced $V_{\text{CUT-IN}}$. On the other hand, etching roughened the anode

Authorized licensed use limited to: J.R.D. Tata Memorial Library Indian Institute of Science Bengaluru. Downloaded on October 04,2022 at 05:20:06 UTC from IEEE Xplore. Restrictions apply.

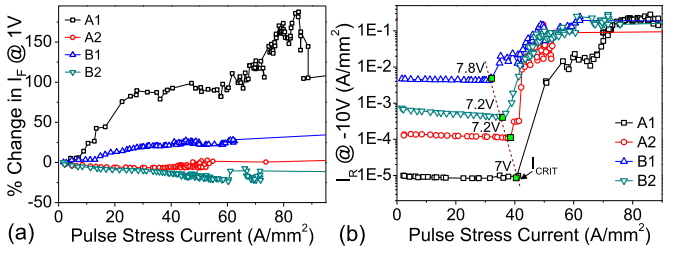

Fig. 5. (a) On-the-fly measured change in forward current and (b) reverse leakage current during high-current stress in the forward conduction mode.

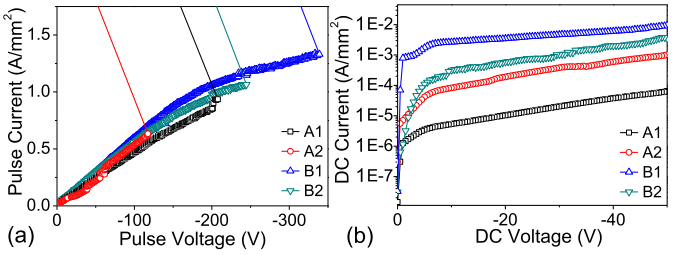

Fig. 6. (a) Pulse *I–V* characteristics of Schottky diode with different anode surface treatments, under high-voltage stress in the reverse blocking regime. (b) DC reverse characteristics of different diode types.

region which translates to an increase in defect density at GaN/metal Schottky interface; D_{it} in diode-B1 by two orders than in an untreated diode-B2. Furthermore, diode-A1 and A2, which had undergone a high-temperature anneal step after recess etching, showed one order lower D_{it} than untreated diode-B2. Rapid thermal annealing (RTA) smoothens the inhomogeneities at the metal/GaN interface and improves SBH from 0.55 to 0.59 eV, which in turn increases specific contact resistance of Schottky diode and leads to higher $V_{\text{CUT-IN}}$, as shown in Fig. 4(b). The change in I_F and I_R that were measured on-the-fly during stress is shown in Fig. 5. I_F showed negligible change in all cases except for diode-A1 where it increased by more than 150%, as shown in Fig. 5(a). The 1.6× higher pulse current in diode-A1 [Fig. 4(a)] leads to an enhanced self-heating and thermionic emission across the Schottky junction, which increases I_F under stress. I_R exhibited significant change but, only beyond a certain critical stress current level, called safe operating stress current (I_{CRIT}) around 7 V in each case, as shown in Fig. 5(b). It depicts that the diode suffers no serious degradation when the stress current is of the order of diode current rating (∼30 A/mm^2 under pulse) or lower. However, the moment the diode encountered current stress greater than its rated current, I_R increased by several orders of magnitude indicating severe degradation, as shown in Fig. 5(b). It is worth noting that irrespective of the initial intrinsic leakage current, all the diodes followed the same trend for I_R change and saturated to 1 mA in each case. These observations highlight that although the Schottky interface influences the failure threshold, $V_{\text{CUT-IN}}$, ON-state resistance; however, the fundamental mechanism responsible for GaN Schottky diode degradation remains unchanged and its failure is universal in nature. It rather strongly depends on the material and device design with weak dependence on the Schottky interface quality.

B. High-Voltage Stress in Reverse Blocking Mode

The diodes were pulse stressed in the reverse blocking mode. Fig. 6 shows the pulse *I–V* characteristics of GaN Schottky diode under high-voltage pulse stress in the reverse blocking mode. All diodes show the linear pulse *I–V* characteristics until the snapback point (V_{TRIG}), followed by an abrupt failure at the snapback. A higher current is observed during the pulse stress than under DC [see Fig. 6(b)]. This is due to the parasitic conduction under pulse stress, which is a strong function of the pulse rise time [13]. Also, the diodes

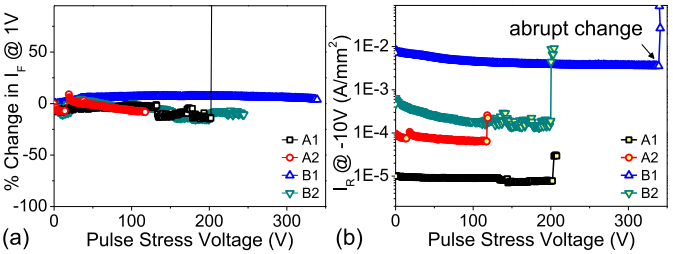

Fig. 7. (a) On-the-fly measured change in forward current and (b) reverse leakage current under high-voltage stress during the reverse blocking state.

show a lower breakdown voltage than under DC due to rapid accumulative degradation under pulse stress [14]. Interestingly, diode-A1 and diode-A2 showed low reverse leakage experienced early failure, whereas diode-B1 with the highest leakage showed maximum V_{TRIG}. These observations point to a pure field-driven failure with a minimal dependence on leakage current density, which is discussed in the subsequent section. The corresponding on-the-fly measurement results are summarized in Fig. 7. Here, I_F remained intact and I_R degraded slightly before seeing an abrupt increase in failure. However, unlike under forward conduction stress, I_R started changing from the very first stress pulse.

V. Analysis and Discussion

In Section IV, it was discovered that irrespective of the type of surface treatment done, GaN diodes degrade in a similar manner while exhibiting similar degradation trends, which points to a common failure mechanism. This section investigates failure physics using one of the diode types (B2).

A. Trap-Assisted Schottky Interface Degradation During High-Current Injection

The cause and coarse of failure in a device can be understood by monitoring the change in its various parameters under stress. The DC characterization of a diode was done at regular intervals during stress. The stress was interrupted at every 20-V increment in stress and DC voltage at anode was swept from −4 to 4 V to record the *I–V* characteristic of the diode. Following this, *C–V* characterization was done and D_{it} was extracted at Schottky interface using the relation given in Section III. Fig. 8 summarizes the results. As shown in Fig. 8(a), Schottky junction turns leaky with gradual increase

Authorized licensed use limited to: J.R.D. Tata Memorial Library Indian Institute of Science Bengaluru. Downloaded on October 04,2022 at 05:20:06 UTC from IEEE Xplore. Restrictions apply.

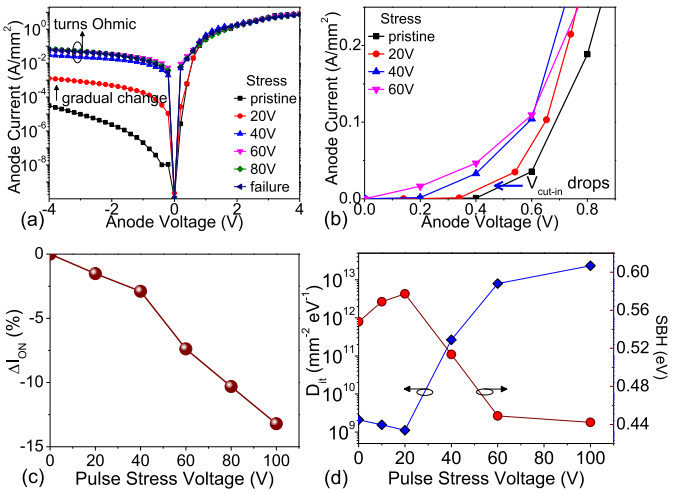

Fig. 8. Change in DC I–V characteristics of diode measured under high-current stress during forward conduction. (a) Increase in reverse leakage current, (b) reduction in $V_{\text{CUT-IN}}$, (c) drop in I_{ON}, and (d) increment in D_{it} with decrease in SBH are measured on-the-fly during stress.

of nearly four orders in reverse leakage current. A closer look at the linear region in forward regime reveals a consistent decrease in $V_{\text{CUT-IN}}$ with increase in stress voltage, as shown in Fig. 8(b). Also, the forward saturation current (at 4 V DC) saw a monotonous drop of ~15% [Fig. 8(c)] with increment in stress. To understand the root cause of these distinct changes, SBH and interface defect density (D_{it}) were monitored during stress. Fig. 8(d) shows the change in D_{it} and SBH recorded in device under stress. As seen, diode under forward conduction stress saw initial drop in D_{it}, which is attributed to thermal annealing of the interface defects by the high stress current [15]. Beyond a certain stress current value, called safe operating stress current (I_{CRIT}), the density of defects at metal/GaN Schottky interface increased by four orders with simultaneous decrease in SBH from 0.56 to 0.44 eV. The lowered SBH leads to the increase in reverse leakage current as shown in Figs. 8(a) and 5(b), following the Schottky diode equation [11]:

$$I_F = I_S\left[e^{\frac{qV}{\eta kT}} - 1\right], \quad I_S = AA^*T^2e^{-\frac{q\phi}{kT}} \tag{1}$$

where I_S is the reverse saturation current, η is the ideality factor, ϕ is the SBH, T is the absolute temperature, k is the Boltzmann constant, A^* is the Richardson constant, and A is the Schottky contact area.

The earlier observations indicate that under forward conduction, the high-current pulse stress increases D_{it} at the metal/GaN Schottky interface. However, it is still not very clear by what mechanism the change in interface defect density alters $V_{\text{CUT-IN}}$ and barrier height. To understand the underlying physics, diode structure was simulated using the well-calibrated TCAD setup explained in our earlier works [16]. Donor- and acceptor-type states are considered at the anode metal/GaN Schottky interface. Shallow donor levels native to N-vacancies are considered with an energy of 60 meV with respect to the conduction band. Acceptor level is believed to originate from Ga-vacancy. In an AlGaN/GaN system, N-displacement (Nitrogen vacancy) requires lower

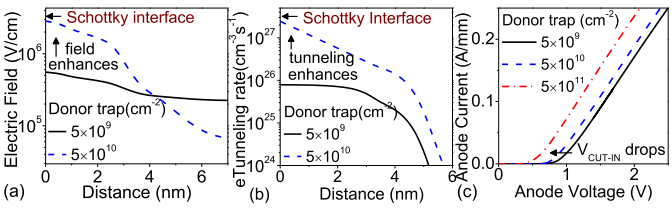

Fig. 9. (a) Electric-field distribution, (b) electron tunneling rate near Schottky contact, and (c) I–V characteristics of Schottky diode simulated for different concentrations of donor traps at metal/GaN Schottky interface.

energy than creating a Ga-vacancy in the lattice [17]. Therefore, an increase in donor trap density at the Schottky interface is favored under forward conduction stress. The diode structure shown in Fig. 2 is simulated at different donor trap concentrations and change in device behavior is studied. Electric field peaks at anode edge. Beside I–V characteristics, the E-field component along the y-direction (as marked in Fig. 2) and the e-Tunneling rate along xy-direction are extracted, as shown in Fig. 9. With one order increment in donor trap density at Schottky interface, the local electric field was found to increase by ten times, as shown in Fig. 9(a). This is attributed to increased charge density at the interface, which increases the field as per Poisson equation [11]

$$E = \int \frac{\rho(x)}{\epsilon} \mathrm{d}x \tag{2}$$

where ρ is the charge density from ionized donor trap states.

Local field enhancement in the Schottky junction's vicinity increases transmission coefficient and augments electron tunneling rate through Schottky barrier, as shown in Fig. 9(b). Moreover, it reduces barrier height as shown in Fig. 8(d), via image force lowering. These changes in barrier consequently enhance carrier emission across Schottky barrier, which is evident from the increase in reverse leakage [see Fig. 8(a)]. The reduced $V_{\text{CUT-IN}}$ at higher donor trap density [see Fig. 9(c)] is a manifestation of lowered SBH. These cascading effects gradually turn Schottky contact into Ohmic.

B. Electromechanical Stress During High Field Reverse Blocking State

Furthermore, the diode's DC characterization was done at regular intervals during high-voltage pulse stress in the reverse blocking state. Fig. 10 shows the change in DC I–V characteristics under stress. As shown in Fig. 10(a), the reverse leakage remained intact until it abruptly increased at the verge of device failure, unlike the case under high-current stress in forward conduction where a gradual change in leakage was noticed. This observation suggests that GaN Schottky diode undergoes gradual/soft failure under high-current stress during forward conduction, whereas it faces abrupt breakdown under high-voltage pulse stress during the reverse blocking state. The linear region of I–V characteristics reveals an unchanged $V_{\text{CUT-IN}}$ and decrease in R_{ON}, which contrast with behavior under high-current forward stress where $V_{\text{CUT-IN}}$ changed and R_{ON} remained intact [Fig. 8(b)]. Furthermore, D_{it} increased linearly with voltage stress, from the very

Authorized licensed use limited to: J.R.D. Tata Memorial Library Indian Institute of Science Bengaluru. Downloaded on October 04,2022 at 05:20:06 UTC from IEEE Xplore. Restrictions apply.

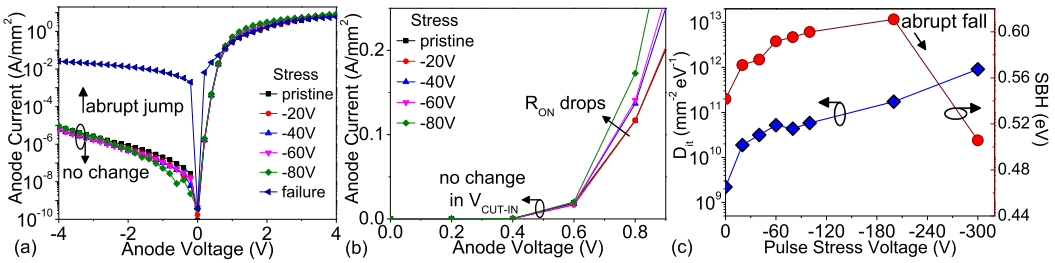

Fig. 10. (a) and (b) Change in DC *I*–*V* characteristics and (c) D_{it} and SBH of diode, measured under high-voltage stress during the reverse blocking mode.

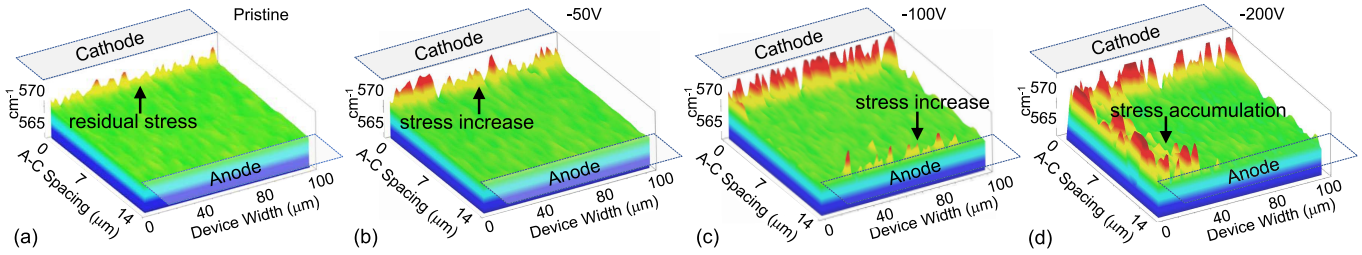

Fig. 11. (a) Raman map captured in drift region between anode–cathode of pristine diode, before high-voltage pulse stress in reverse blocking state. This reveals residual compressive strain at cathode edge. On-the-fly Raman map was captured after reverse blocking state stress of (b) −50, (c) −100, and (d) −200 V. With increasing reverse bias voltage stress, compressive stress accumulates at edge and corner(s) of recessed anode.

beginning unlike that under current stress in the forward mode, as shown in Fig. 10(c). This took place, however, at a much slower rate compared to that under high-current stress in forward conduction [Fig. 8(d)]. Surprisingly, despite the D_{it} increment, a constant increase in SBH is noticed. A similar trend is noticed in all cases, irrespective of type of anode surface treatment. Considering these observations, it can be said that D_{it} increment alone cannot explain the diode failure under high-voltage pulse stress during the reverse blocking mode, and possibly, there exists a different failure physics.

It should be noted that the GaN/AlGaN material system possesses intrinsic piezoelectric nature. To account for this aspect, the evolution of mechanical strain in diode is captured on-the-fly during pulse stress using 2-D Raman spectroscopy. All maps are referenced to GaN's Raman peak, E_{2-H} (567.5 cm^{-1}). Fig. 11 shows the evolution of mechanical strain in the anode–cathode region of diode during reverse blocking pulse stress. The Raman map of pristine device as shown in Fig. 11(a) reveals residual compressive strain present at cathode, which possibly originates from coefficient of thermal expansion (CTE) mismatch between cathode metal stack (Ti/Al/Ni/Au) and underlying GaN/AlGaN, after post-metal deposition anneal. The 2-D Raman maps shown in Fig. 11(b)–(d) reveal that in the reverse blocking mode, with an increase in pulse stress voltage, the compressive strain builds up in the drift region, at edges and corners of recessed anode. This explains why failure occurred at recess edges in diodes during reverse blocking state, as discussed in Section VI. Therefore, failure of GaN Schottky diode under high-voltage pulse stress in the reverse blocking mode is governed by the piezoelectric stress distribution and hence should follow a field-dependent failure mechanism as discussed next.

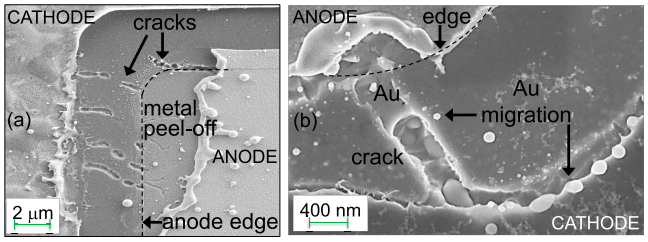

Fig. 12. SEM analysis of diodes which failed under high-current stress during forward conduction depicting (a) multiple cracks and metal peel-off at anode edge and (b) metal migration via cracked region.

VI. Failure Analysis

After stress testing, failure analysis of damaged regions of diodes was done to gain physical insight into the degradation mechanism(s). Based on the discussion in Section V and results obtained from failure analysis, the physics of failure in AlGaN/GaN-based Schottky diodes under transient pulse stress is proposed.

A. Failure Under High-Current Stress

Fig. 12 shows the post-failure SEM micrographs of devices which failed under high-current stress in forward conduction. Multiple cracks originated from anode end, which propagated toward cathode contact. The contact metal at anode edge peeled off and folded. These signatures reveal the thermal nature of failure [18] and are possibly caused by the high current flow after Schottky junction turns Ohmic. Based on these observations and discussion from the previous section, the following failure mechanism is presented, as shown in Fig. 13. During forward conduction, anode gets stressed, while the cathode is grounded. The peak electric field lies at the metal/GaN Schottky junction [Fig. 9(a)]. At high

Authorized licensed use limited to: J.R.D. Tata Memorial Library Indian Institute of Science Bengaluru. Downloaded on October 04,2022 at 05:20:06 UTC from IEEE Xplore. Restrictions apply.

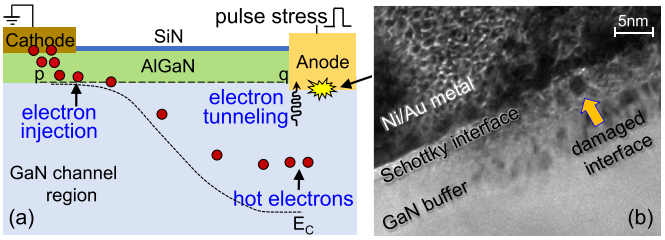

Fig. 13. (a) Device schematic illustrating various events under high-current stress during forward conduction in AlGaN/GaN recessed Schottky diode. The conduction band edge as shown is plotted along line *p*–*q* in the channel region. (b) Cross-sectional TEM image of anode region of a Schottky diode which failed under high-current stress during forward conduction.

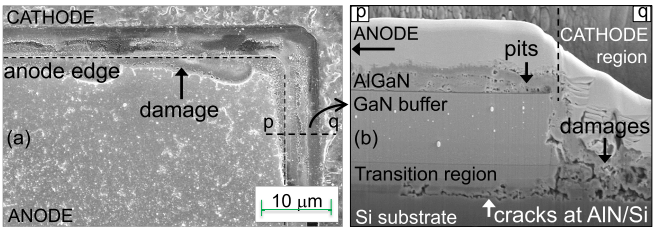

Fig. 14. (a) SEM image of diode which failed under high-voltage stress during the reverse blocking state. (b) Cross-sectional SEM image of damaged region taken along line *p*–*q* as marked in (a).

channel field, 2DEG electrons get hot and they can take two possible routes as shown in Fig. 13(a) such as electrons tunnel through Schottky barrier to reach anode contact as clear from significant tunneling rate in Fig. 9(b) and electrons impinge on metal/GaN junction and damage/modify the Schottky interface as clear from cross-sectional TEM of damaged anode region shown in Fig. 13(b). It should be noted that the CTE mismatch between GaN and anode metals (Ni/Au) introduces additional thermoelastic residual strain at the Schottky interface, making it more vulnerable to damage. The hot energetic electrons create nitrogen vacancy in GaN at and around the Schottky interface which gets reflected by increased D_{it} (donor type), as shown in Fig. 8(d). Increment in donor traps result in local electric-field enhancement at Schottky junction [see Fig. 9(a)], which boosts electron tunneling [see Fig. 9(b)], lowers SBH [see Fig. 8(d)] and reduces $V_{CUT\text{-}IN}$ [see Figs. 8(b) and 9(c)]. Consequently, reverse leakage increases, which gradually turns Schottky contact to Ohmic. Once the Schottky junction is completely vanished (turns Ohmic) at the snapback point, device current increases abruptly, only limited by measurement system's loadline and voltage across device drops to a low value. Finally, at high current in a snapback region, thermal failure occurs in device leading to cracking in top AlGaN/GaN layers, melting/ folding of anode metals (see Fig. 12). EDX analysis confirms that Au (14%) melts and migrated from anode to cathode via crack [see Fig. 12(b)].

B. Failure Under High-Voltage Stress

Fig. 14 shows the post-failure SEM and HR-TEM analysis of damaged regions of a diode failed under high-voltage stress during the reverse blocking state. The damage occurred in a drift region and at anode recess edge with anode contact metal blown-off and no signs of metal melting observed. The absence of metal melting/folding in damaged regions reveals the nonthermal nature of the failure and points to a field-dependent mechanism. A cross-sectional SEM image takes along the line *p*–*q* [shown in Fig. 14(a)] in diode's drift region reveals massive damage under the cathode contact with the formation of pits. Moreover, cracking of AlGaN/GaN epilayer can be seen, which occurred at the transition region and substrate interface. The cracks propagated from cathode to anode creating a parasitic current flow path. These cracks provide a low-resistance path for carrier transport as well as low-energy path for material diffusion [19]. This decreases the effective R_{ON} of diode under stress [Fig. 10(b)]. Development of such cracks close to Si-substrate also highlights the presence of high residual strain at transition region/substrate interface [13]. Moreover, pits and defects at multiple locations across the AlGaN barrier were also seen. Based on these observations and results from the previous sections, the following mechanism can explain the diode failure under high-voltage pulse stress in the reverse blocking state; with an increase in negative stress voltage at anode, the depletion region extends toward the cathode and the electric field at cathode increases. E-field has a horizontal component (E_x) along the device surface and vertical component (E_z) normal to the device surface. E_z introduces piezoelectric strain in GaN [12]. It is worth mentioning that the AlGaN layer also possesses residual tensile strain, due to which elastic energy constantly increases with the electric field at cathode. This behavior has been captured by Raman spectroscopy, as shown in Fig. 11. Beyond a critical value, the release of elastic energy causes the creation of crystallographic defects/pits in AlGaN/GaN and cracks at the transition region/substrate interface, as shown in Fig. 14(b). Cracks offer low resistance for carrier transport, which results in an abrupt increase in diode current leading to snapback in the reverse blocking state.

C. Variability Seen in Failure Thresholds: Dislocation Induced Failure

The lattice mismatch between GaN and underlying Si-substrate gives rise to dislocations that pierce all the way through different layers of AlGaN/GaN epistack and terminate into pits at the device surface. Pits/dislocations if present in the active region of device act as parasitic leakage paths and assist in material diffusion [20], which can result in device failure as the defect density increases. Defect density is never the same across the wafer, and device-to-device variation is bound to happen in MOCVD grown epilayers. Fig. 15 shows the post-failure SEM of diodes which failed when subjected to pulse overstress. In one case, the presence of a dislocation was discovered at anode edge, which shunted the current at high voltages and developed a localized damage, as shown in Fig. 15(a). In another case, a network of pits presents in drift region nucleated cracks, as shown in Fig. 15(b). The pits locally weaken the material via diffusion and electrochemical reactions [20], which resulted in the development of cracks under high fields and eventual failure. Attributed to this behavior and observed role of pits, a device-to-device variation

Authorized licensed use limited to: J.R.D. Tata Memorial Library Indian Institute of Science Bengaluru. Downloaded on October 04,2022 at 05:20:06 UTC from IEEE Xplore. Restrictions apply.

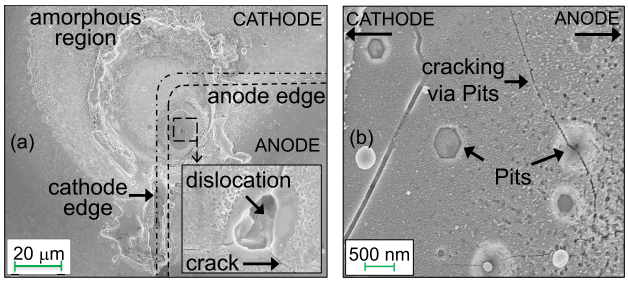

Fig. 15. (a) SEM image of damaged drift region between anode and cathode of a diode. Magnified view shown in inset reveals a dislocation present at anode edge. (b) Image of another failed diode, showing a network of pits/dislocations which provided path for crack propagation.

in dislocation density is naturally bound to cause device-to-device variation in failure threshold. However, as discussed so far, the underlying physical mechanism responsible for failure under pulse stress remains the same.

VII. Conclusion

Reliability physics of AlGaN/GaN recessed Schottky diode is investigated under high-current injection and high-voltage transient stress during forward conduction and reverse blocking state, respectively. Unlike what has been often observed under DC stress, distinct failure mechanisms were discovered under pulse stress. On-the-fly measured diode DC leakage current is an efficient parameter to monitor degradation, both in the forward conduction and reverse blocking mode. Micro-Raman spectroscopy allowed probing piezoelectric stress profile across active regions of diode. Dependence of diode failure mechanism on the intrinsic interface quality is found to be very weak, and all the diode variants despite having different D_{it} and leakage current exhibited similar degradation trends. In the forward mode, diode is found to be reliable in a low-current regime; however, it is extremely unreliable in high-current domain and suffers severe degradation under overcurrent stress. Under high-current injection in the forward mode, the hot electrons create donor-type N-vacancy in the GaN region at the Schottky interface. TCAD analysis revealed that an increase in donor trap concentration increased ionized trap charge density at the Schottky junction and in its vicinity. This led to electric-field enhancement, which boosted electron tunneling across the Schottky barrier. This, with repeated stress and gradual degradation, eventually turned Schottky interface to Ohmic, which was confirmed by four orders of increase in DC leakage current and significantly lowered SBH post-stress. On the other hand, high-voltage stress in the reverse blocking state caused piezoelectric stress at recessed anode edge and strain accumulation with repeated stress. This triggered failure at anode corners. While failure was found to be gradual under forward conduction stress, it was, however, abrupt under reverse blocking mode. Failure analysis performed using SEM, TEM, and EDX corroborate well with electrical, optical, and Raman-based findings.

References

[1] A. Soni, S. Shikha, and M. Shrivastava, "On the role of interface states in AlGaN/GaN Schottky recessed diodes: Physical insights, performance tradeoff, and engineering guidelines," *IEEE Trans. Electron Devices*, vol. 66, no. 6, pp. 2569–2576, Jun. 2019, doi: 10.1109/TED.2019.2912783.

[2] A. N. Tallarico *et al.*, "ON-state degradation in AlGaN/GaN-on-silicon Schottky barrier diodes: Investigation of the geometry dependence," *IEEE Trans. Electron Devices*, vol. 63, no. 9, pp. 3479–3486, Sep. 2016, doi: 10.1109/TED.2016.2593945.

[3] J. Hu *et al.*, "Time-dependent breakdown mechanisms and reliability improvement in edge terminated AlGaN/GaN Schottky diodes under HTRB tests," *IEEE Electron Device Lett.*, vol. 38, no. 3, pp. 371–374, Mar. 2017, doi: 10.1109/LED.2017.2661482.

[4] J. Hu *et al.*, "Investigation of constant voltage off-state stress on au-free AlGaN/GaN Schottky barrier diodes," *Jpn. J. Appl. Phys.*, vol. 54, no. 4, Apr. 2015, Art. no. 04DF07, doi: 10.7567/jjap.54.04df07.

[5] E. Acurio *et al.*, "Reliability improvements in AlGaN/GaN Schottky barrier diodes with a gated edge termination," *IEEE Trans. Electron Devices*, vol. 65, no. 5, pp. 1765–1770, May 2018, doi: 10.1109/TED.2018.2818409.

[6] H. Kang *et al.*, "Effects of a GaN cap layer on the reliability of AlGaN/GaN Schottky diodes," *Phys. Status Solidi*, vol. 212, no. 5, pp. 1158–1161, May 2015. [Online]. Available: https://onlinelibrary.wiley.com/doi/abs/10.1002/pssa.201431719

[7] S. Xue, F. Gao, W. Sun, and B. Li, "Protection principle for a DC distribution system with a resistive superconductive fault current limiter," *Energies*, vol. 8, no. 6, pp. 4839–4852, 2014. [Online]. Available: https://www.mdpi.com/1996-1073/8/6/4839/htm

[8] A. J. Collin and S. Z. Djokic, "Voltage disturbances and inrush current of DC power supplies," *Renew. Energy Power Qual. J.*, vol. 1, no. 8, pp. 869–875, 2010.

[9] B. Shankar *et al.*, "Trap assisted stress induced ESD reliability of GaN Schottky diodes," in *Proc. 40th Electr. Overstress/Electrostatic Discharge Symp. (EOS/ESD)*, Sep. 2018, pp. 1–6, doi: 10.23919/EOS/ESD.2018.8509745.

[10] M. Rashid, *Power Electronics Handbook: Devices Circuits and Application*. Amsterdam, The Netherlands: Elsevier, 2011.

[11] S. M. Sze, *Physics of Semiconductor Devices*. Hoboken, NJ, USA: Wiley, 2007.

[12] A. Sarua *et al.*, "Piezoelectric strain in AlGaN/GaN heterostructure field-effect transistors under bias," *Appl. Phys. Lett.*, vol. 88, no. 10, Mar. 2006, Art. no. 103502, doi: 10.1063/1.2182011.

[13] B. Shankar *et al.*, "Time dependent early breakdown of AIGaN/GaN Epi stacks and shift in SOA boundary of HEMTs under fast cyclic transient stress," in *IEDM Tech. Dig.*, Dec. 2018, p. 34, doi: 10.1109/IEDM.2018.8614690.

[14] B. Shankar, A. Soni, H. Chandrasekar, S. Raghavan, and M. Shrivastava, "First observations on the trap-induced avalanche instability and safe operating area concerns in AlGaN/GaN HEMTs," *IEEE Trans. Electron Devices*, vol. 66, no. 8, pp. 3433–3440, Aug. 2019, doi: 10.1109/TED.2019.2919491.

[15] S. Singhal *et al.*, "GaN-ON-Si failure mechanisms and reliability improvements," in *Proc. IEEE Int. Rel. Phys. Symp.*, Mar. 2006, pp. 95–98, doi: 10.1109/RELPHY.2006.251197.

[16] V. Joshi, A. Soni, S. P. Tiwari, and M. Shrivastava, "A comprehensive computational modeling approach for AlGaN/GaN HEMTs," *IEEE Trans. Nanotechnol.*, vol. 15, no. 6, pp. 947–955, Nov. 2016, doi: 10.1109/TNANO.2016.2615645.

[17] D. C. Look, G. C. Farlow, P. J. Drevinsky, D. F. Bliss, and J. R. Sizelove, "On the nitrogen vacancy in GaN," *Appl. Phys. Lett.*, vol. 83, no. 17, pp. 3525–3527, Oct. 2003, doi: 10.1063/1.1623009.

[18] B. Shankar and M. Shrivastava, "Safe operating area of polarization super-junction GaN HEMTs and diodes," *IEEE Trans. Electron Devices*, vol. 66, no. 10, pp. 4140–4147, Oct. 2019, doi: 10.1109/TED.2019.2933362.

[19] B. Shankar, S. Raghavan, and M. Shrivastava, "ESD reliability of AlGaN/GaN HEMT technology," *IEEE Trans. Electron Devices*, vol. 66, no. 9, pp. 3756–3763, Sep. 2019, doi: 10.1109/TED.2019.2926781.

[20] M. Kuball, M. Ťapajna, R. J. T. Simms, M. Faqir, and U. K. Mishra, "AlGaN/GaN HEMT device reliability and degradation evolution: Importance of diffusion processes," *Microelectron. Rel.*, vol. 51, no. 2, pp. 195–200, Feb. 2011.

Authorized licensed use limited to: J.R.D. Tata Memorial Library Indian Institute of Science Bengaluru. Downloaded on October 04,2022 at 05:20:06 UTC from IEEE Xplore. Restrictions apply.